Mercury isotopic constraints on mercury cycling across a permafrost thaw gradient in Stordalen Mire

M.F. Fahnestock[1], J.G. Bryce[1], C.T. Driscoll[2], B. Garvey[1], V.I. Rich[3], R.K. Varner[1,4]

[1]Department of Earch Sciences, University of New Hampshire, Durham, NH ; [2]Department of Civil and Environmental Engineering, Syracuse University, Syracuse, NY; [3]Department of Microbiology, The Ohio State University, Columbus, OH; [4]Institute for the Study of Earth, Oceans and Space, University of New Hampshire, Durham.

Introduction

Figure 1. Map of Hg in Arctic soils (Schuster et al., 2018) and permafrost delineations of current and projected (for 2100) permafrost extent, according to Representative Concentrations Pathway (RCP) scenarios 4.5 and 8.5 from IPCC fifth assesment report (Slater and Lawrence, 2013; AMAP, 2013). Yellow/blue star denotes study site location.

Credit: http://www.grida.no/resources/13344; Philippe Rekacewicz and Nieves Lopez Izquierdo

Mercury in the soil from 0 to 300 cm
mg Hg/m^2
5 to 20 · 20 to 80 · 80 to 150 · More than 150
RCP 4.5 · RCP 8.5 · Current extent of permafrost

- Permafrost constitutes the largest long-term Hg reservoir, containing twice as much Hg as oceans, the atmosphere and all other soils combined (Schuster et al., 2018).
- Warming global temperatures, particularly in the Arctic, drives permafrost thaw that threatens to release previously sequestered Hg back into the atmosphere and hydrosphere.
- Isotopes of Hg enable the deciphering of the major pathways controlling Hg biogeochemical cycling and may provide insight into key mechanisms significant to Hg distribution aross a permafrost thaw gradient.

Background

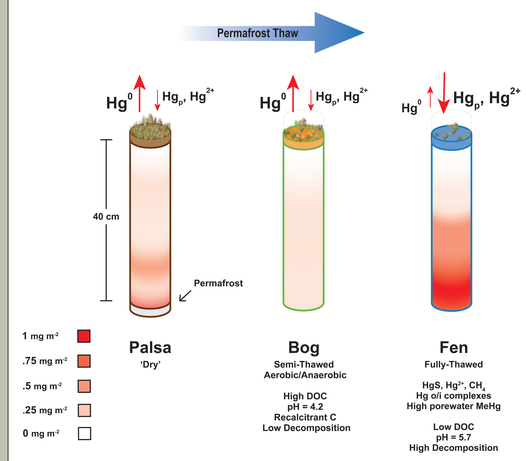

Figure 2. Schematic of Hg biogeochemical cycling across permafrost thaw with emphasis on major Hg pools and pathways. Red arrows denote gaseous (Hg^0) flux for each stage of the thaw sequence. Peat inventories (total Hg) correspond to the top 40 cm of the mire surface (cf. legend for corresponding range) from Fahnestock et al. (2019).

Methods

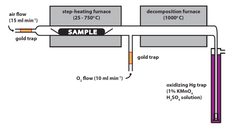

Figure 3 a) Samples underwent Hg extraction via two-stage combustion furnace and subsequent oxidation into a $KMnO_4$ trap as described in Biswas et al. (2008).

b) Schematic of Hg extraction apparatus.

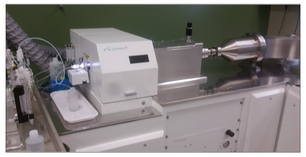

Figure 4. Once extracted and concentrated, Hg is reduced with stannous chloride and introduced via a cold-vapor generation apparatus (CETAC HGX-200) into a nu instruments plasma II.

Study Site & Design

Figure 5. Observed landscape evolution due to permafrost thaw over thirteen years at Stordalen Mire.

Photo Credit: S. Burke & P.M. Crill

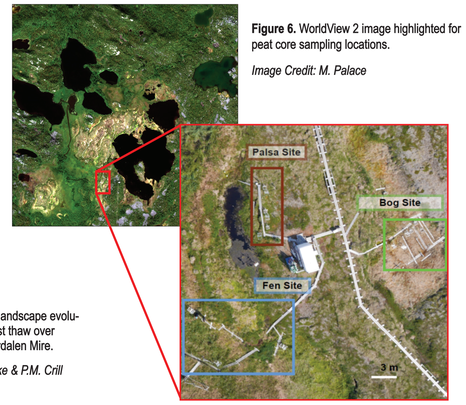

Figure 6. WorldView 2 image highlighted for peat core sampling locations.

Image Credit: M. Palace

- Stordalen Mire is a well characterized multidisciplinary research site located at the edge of the discontinuous permafrost zone where permafrost thaw has been documented since 1940.
- The four habitat types in this study include: (1) Palsa - hummocks underlain by permafrost, (2) Bog - partially thawed *Sphagnum spp.* dominated, (3) Fen - fully-thawed and dominated by *Eriophorum*, and (4) Three post-glacial lakes.

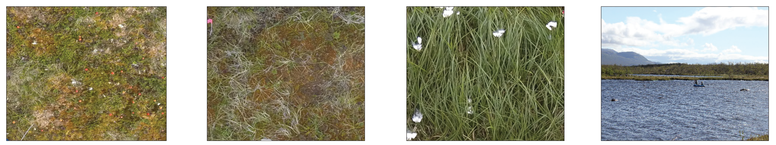

Figure 7. Habitats represented at Stordalen Mire. *Photo Credit: M.F. Fahnestock*

- **Isotopic signatures support with the Fahnestock et al. (2019) conceptual model of paslt to bog thaw transition marked by Hg evasion, presumably from photochemical reduction.**

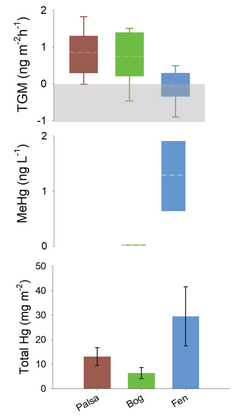

Figure 8. Summary of Hg results from Fahnestock et al. (2019). From top to bottom: mean total gaseous Hg flux, porewater Methyl Hg (MeHg) concentrations in Bog and Fen and total Hg in peat corrected for peat density.

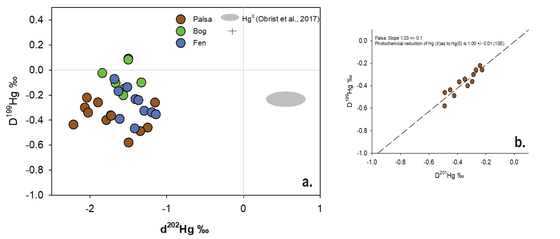

Figure 9 a) Links between mass-dependent (MDF) and mass independent (MIF) Hg isotope fractionation presented as δ^{202}Hg and Δ^{199}Hg, respectively. **a)** Hg isotopes in the bog shows are more positive Δ^{199}Hg. Although wet deposition was not measured at this site it generally tends to be a wide range of values but generally positive Δ^{199}Hg and near-zero δ^{202}Hg. Therefore, the bog may be experiencing a mixture of wet deposition inputs. The Fen sediment Hg isotope signatures imply Hg accumulation from multiple pathways including both wet/dry deposition and via inputs from the surrounding palsa. (Analytical 2SE noted by + symbol in legend) **b)** The palsa shows a relationship with photochemical reduction of Hg which is consistent with interpretations from Fahnestock et al., 2019.

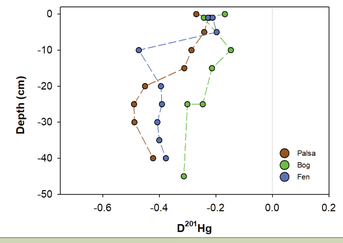

Figure 10. Depth profiles of Δ^{201}Hg across the thaw gradient shows distinct variations across sites and with depth. The bog show the least variation with depth consistent with total Hg depth profiles of total Hg in previous study. Analytical 2SE within symbol unless noted.

- **Lake sediment Hg isotopic signatures suggest each lake may be experiencing different key controls on Hg cycling related to chemical and physical lake properties.**

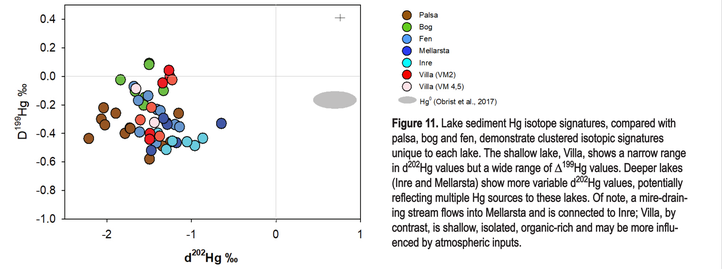

Figure 11. Lake sediment Hg isotope signatures, compared with palsa, bog and fen, demonstrate clustered isotopic signatures unique to each lake. The shallow lake, Villa, shows a narrow range in δ^{202}Hg values but a wide range of Δ^{199}Hg values. Deeper lakes (Inre and Mellarsta) show more variable δ^{202}Hg values, potentially reflecting multiple Hg sources to these lakes. Of note, a mire-draining stream flows into Mellarsta and is connected to Inre; Villa, by contrast, is shallow, isolated, organic-rich and may be more influenced by atmospheric inputs.

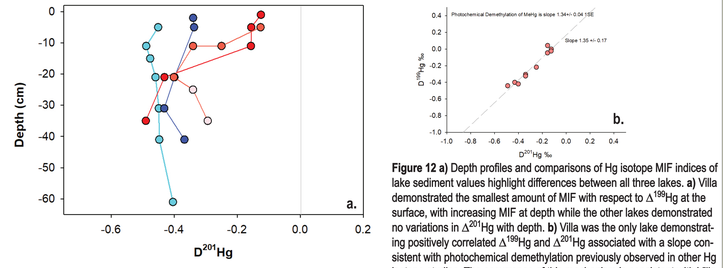

Figure 12 a) Depth profiles and comparisons of Hg isotope MIF indices of lake sediment values highlight differences between all three lakes. **a)** Villa demonstrated the smallest amount of MIF with respect to Δ^{199}Hg at the surface, with increasing MIF at depth while the other lakes demonstrated no variations in Δ^{201}Hg with depth. **b)** Villa was the only lake demonstrating positively correlated Δ^{199}Hg and Δ^{201}Hg associated with a slope consistent with photochemical demethylation previously observed in other Hg isotope studies. The occurrence of this mechanism is consistent with Villa containing low surface water MeHg abundances but high sediment Hg.

Summary

- Results from peat and lake sediments showed variations in both MDF and MIF across all sites and in most cases varied with depth.
- The Δ^{199}Hg/ Δ^{201}Hg from the shallow lake Villasjön, together with low surface water methyl Hg contents, suggest that the paired chemical signatures may be explained by photochemical demethylation of MeHg being an important control on Hg cycling in this lake but less so for the other two lakes in this study
- Vegetation samples taken this past July 2019 will be useful in identifying differences between atmospheric-vegetation fractionation pathways across the palsa, bog and fen.

Acknowledgments

This work was funded by NSF-12555888 (JGB), the Northern Ecosystems Research for Undergraduates NSF-1063037 (RKV), Graduate Research Awards from UNH Earth Sciences and the Geological Society of America, the Iola Hubbard Climate Change Endowment and by the Genomic Science Program of the United States DOE Office of Biological and Environmental Research, DE-SC0016440. We thank the Abisko Scientific Research Station and the Climate Change Impacts Centre of Umeå University for providing infrastructure and logistical support, in particular, Dr. R. Giesler. We also thank Dr. S. Frey, M. Knorr and Drs. J. Johnson, Phillips and Setera for assistance with sample prep and CNS analyses, Drs. J. Blum and M. Johnson for assisntance in implimentation of isotope extractions, M. Montesdeoca for MeHg analysis and Dr. P.M. Crill for project development feedback. A very special thanks to R. U. Fahnestock for graphic design assistance.

References

AMAP, 2013, Global Mercury Modellng: Update of Modelling Results in the Global Mercury Assessment.

Biswas, A. et al. (2008) Natural mercury isotope variation in coal deposits and organic soils. Env. Sci. Technol. 42, 8303–8309.

Fahnestock, M.F. et al., (2019) Mercury reallocation in thawing subarctic peatlands. GPL, 11, doi: 10.7185/geochemlet.1922

Obrist, D. et al. (2017) Tundra uptake of atmospheric elemental mercury drives Arctic mercury pollution. Nature 547, 201–204.

Schuster, P. F. et al. (2018) Permafrost Stores a Globally Significant Amount of Mercury. Geophys. Res. Lett. 45, 1463–1471.

Slater, A.G. and Lawrence, D.M. (2013) Diagnosing present and future permafrost from climate models, J. of Clim. 26 (15), p.5608-5623.